

# THE DYNAMICS EXPLORER LANGMUIR PROBE INSTRUMENT

J. P. KREHBIEL

*Applied Engineering Division Goddard Space Flight Center, Greenbelt, Maryland 20771, U.S.A.*

L. H. BRACE and R. F. THEIS

*Laboratory for Planetary Atmospheres, Goddard Space Flight Center, Greenbelt, Maryland 20771, U.S.A.*

W. H. PINKUS

*Department of Atmospheric and Oceanic Sciences, University of Michigan,  
Ann Arbor, Michigan 48105, U.S.A.*

and

R. B. KAPLAN

*Ultramet, Incorporated, Pacoima, California, U.S.A.*

(Received 22 July, 1981)

**Abstract.** The Dynamics Explorer Langmuir probe instrument (DE-LANG) has been designed to perform *in-situ* measurements of electron temperature and electron and ion density in the Earth's ionosphere. It is a former spare unit from the Pioneer Venus mission that has been modified to interface with the DE spacecraft. Two independent sensors are connected to individual adaptive sweep voltage circuits which continuously track the changing electron temperature and spacecraft potential while autoranging electrometers adjust their gain in response to the changing plasma density. The control signals used to achieve this automatic tracking provide a continuous monitor of the ionospheric parameters without telemetering each volt-ampere curve. Additionally, internal data storage circuits permit high resolution, high data rate sampling of selected volt-ampere curves for transmission to the ground to verify or correct the inflight processed data. The availability of analog telemetry channels in the DE spacecraft permits the transmission of raw electro-meter data from either of the two sensors. These analog outputs also provide high resolution measurements of electron or ion density from either sensor when fixed positive or negative potentials are applied.

## 1. Introduction

The Dynamics Explorer Langmuir probe instrument (DE-LANG) on the DE-B spacecraft will provide measurements of electron temperature ( $T_e$ ), electron and ion densities ( $N_e$  and  $N_i$ ) and spacecraft potential ( $V_s$ ). In the interest of minimizing cost, an existing unit, originally a spare for the Pioneer Venus Orbiter Electron Temperature Probe [1], has been adapted to suit the DE mission. The purpose of this paper is to outline the measurement technique, illustrate its adaptation to DE, and describe the operational modes and data formats.

## 2. Theory of the Method

Irving Langmuir and H. Mott-Smith, Jr., first reported the use of an electrostatic probe in a laboratory plasma in 1924 [2]. This cylindrical probe technique, now often referred to as a Langmuir probe, has been used extensively to characterize the Earth's iono-

sphere [3, 4] and the ionosphere of Venus [5–8]. Langmuir probe theory and application have been widely reported in the literature [1–12]. Here it will suffice to provide a brief description of the technique. A theoretical volt-ampere curve is shown in Figure 1 to illustrate the method. The curve represents the sum of the ion and electron currents,  $I_i$  and  $I_e$ , collected from the ionospheric plasma surrounding the sensor. The curve begins in the ion saturation region where the probe potential is sufficiently negative to prohibit plasma electrons from reaching it. At this point, current to the probe is due primarily to ions. In the retardation region, where the probe potential is less negative, some of the ionospheric electrons overcome the potential and produce an exponentially increasing current.  $T_e$  determines the power of the exponential, with lower  $T_e$  yielding a narrower retarding region. In the electron saturation region, the probe is positive with respect to the plasma and thus attracts electrons. Equations appropriate to the three regions of the curve are given below.

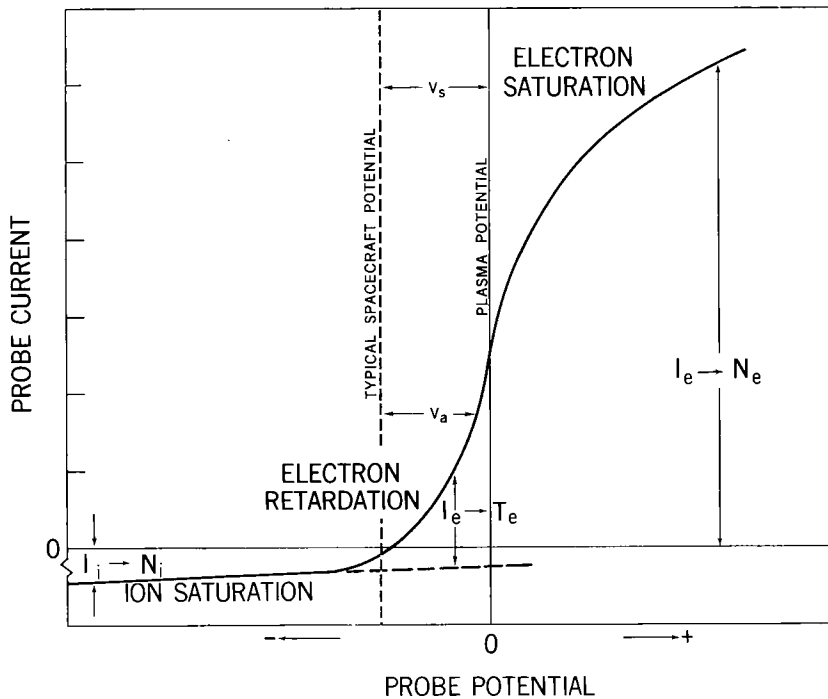


Fig. 1. A theoretical volt-ampere characteristic of a cylindrical collector in a plasma showing the regions of the curve from which  $N_i$ ,  $T_e$ ,  $N_e$ , and  $V_s$  may be calculated. Note: The current scale in the ion saturation region is enlarged for illustrative purposes.

In the ion saturation region, with the sensor axis normal to the velocity vector, the ion current is given by [9]

$$I_i = AN_e w / \pi (1 + kT_e / m_i w^2 + 2eV / m_i w^2)^{1/2}. \quad (1)$$

In the electron retardation region the electron current is given by [10, 11]

$$I_e = AN_e e (kT_e / 2\pi m_e)^{1/2} \exp(eV/kT_e). \quad (2)$$

In the electron saturation region the electron current is given by [1, 11]

$$I_e = (AN_e e / \pi) (2eV/m_e)^{1/2}, \quad (3)$$

where

- $N_e$  electron density;
- $N_i$  ion density;
- $T_e$  electron temperature;
- $T_i$  ion temperature;
- $A$  collector surface area;
- $w$  collector speed with respect to plasma;
- $k$  Boltzmann constant;
- $m_i$  mean ion mass;
- $m_e$  electron mass;
- $V$  collector voltage with respect to the plasma;
- $e$  electron charge.

Langmuir probe measurements are always made with respect to the spacecraft potential,  $V_s$ . As can be seen in Figure 1,  $V_s$  adds a bias in series with the applied  $V_A$ . Thus the  $V$  in Equations (1), (2), and (3) is modulated by  $V_s$ . It is therefore necessary to take special steps in spacecraft design to assure a stable value of  $V_s$  near zero V. The use of a fairly uniform external conductive surface of the spacecraft and a negative (positive ground) solar array is expected to provide the needed stability. The DE-LANG is designed to accommodate residual changes in  $V_s$  and to operate fully over a range of  $-5 \text{ V} \leq V_s \leq +5 \text{ V}$  and with reduced effectiveness at up to five additional volts of  $V_s$ .

### 3. The Experimental Arrangement

Design of the Langmuir probe instrument has evolved over more than two decades of spaceflight experience. The present instrument is capable of adaptive operation in which the electronics automatically adjusts the sweep voltage waveform and the electrometer sensitivity. This permits the system to respond in real time to changes in the ionospheric plasma, thus maximizing the resolution and accuracy of the measurements. In the following discussion, the instrument is described in two parts; that which interacts with and measures the plasma environment and that which allows command control of the operational modes and preprocesses the data before telemetry to Earth.

The flight hardware consists of two cylindrical sensors mounted on triaxial booms, their support hardware, and the central electronics. Figure 2 is an illustration of the sensors in place on the nadir ( $-Y$ ) and zenith ( $+Y$ ) pointing faces of the spacecraft structure. Note that the cylindrical axes of both sensors are oriented perpendicular to the velocity vector and as far from booms and antennas as feasible.

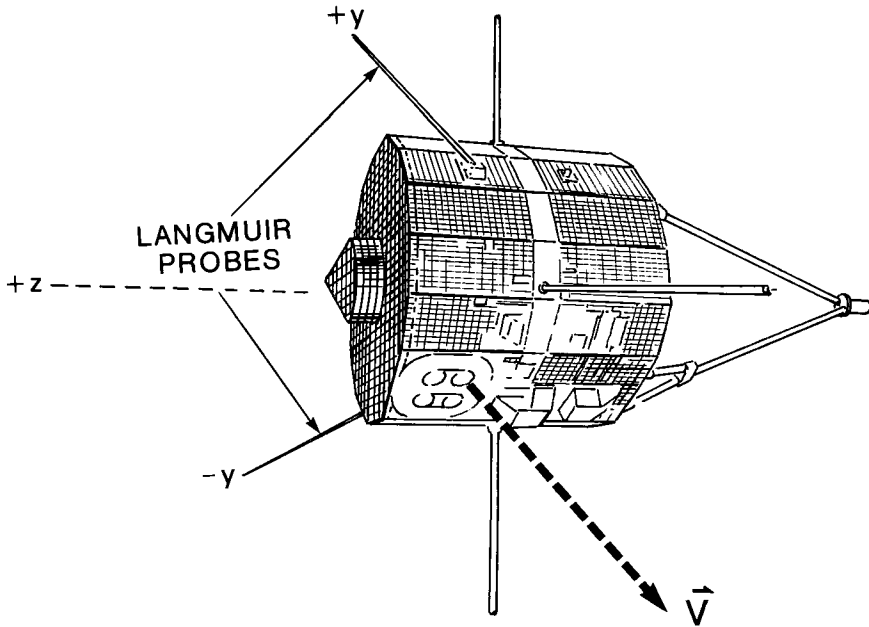


Fig. 2. Langmuir probe mounting locations on the DE spacecraft. The despun spacecraft (one revolution per orbit) will provide both sensors with an unobstructed forward looking view of the incoming plasma.

### 3.1. THE SENSORS AND THE ADAPTIVE CIRCUITRY

The accuracy of the temperature measurements is affected by the characteristics of the sensor surface [12]. In particular, the work function of different crystal surfaces can vary by as much as several tenths of a volt and thereby introduce an uncertainty in the value of  $V$  in (1)–(3). To reduce this error the collectors were fabricated using a chemical vapor deposition (CVD) process. Studies of CVD rhenium show that rhenium deposited by the pyrolytic decomposition of rhenium pentachloride ( $\text{ReCl}_5$ ) exhibits a very high degree of crystal orientation. Rhenium deposited in this manner exhibits a (0001) preferred orientation perpendicular to the plane of growth [13]. Cylindrical tubes of this type have yielded uniform vacuum work functions of 5.1 eV. Molybdenum deposited from  $\text{MoCl}_6$  also shows a very high degree of crystal orientation. Thus both elements become candidates for sensor materials with selection of the particular flight sensors based on metallurgical examination of the crystal structure of more than twenty available sensors. The actual flight collectors have not been selected at the time of this writing.

Each sensor is connected to a dedicated linear electrometer amplifier and its associated  $V_A$  generator. This circuitry is designed to automatically translate ionospheric volt-ampere curves such as those shown in Figure 3 into the best approximation to a properly 'framed' curve, thus permitting optimum determination of the parameters to be measured. The theoretical curve of Figure 1 is presented without defined voltage and current scales, since it is by the determination of these scales that the measurements of  $N_i$ ,  $T_e$ , and  $N_e$  are made.

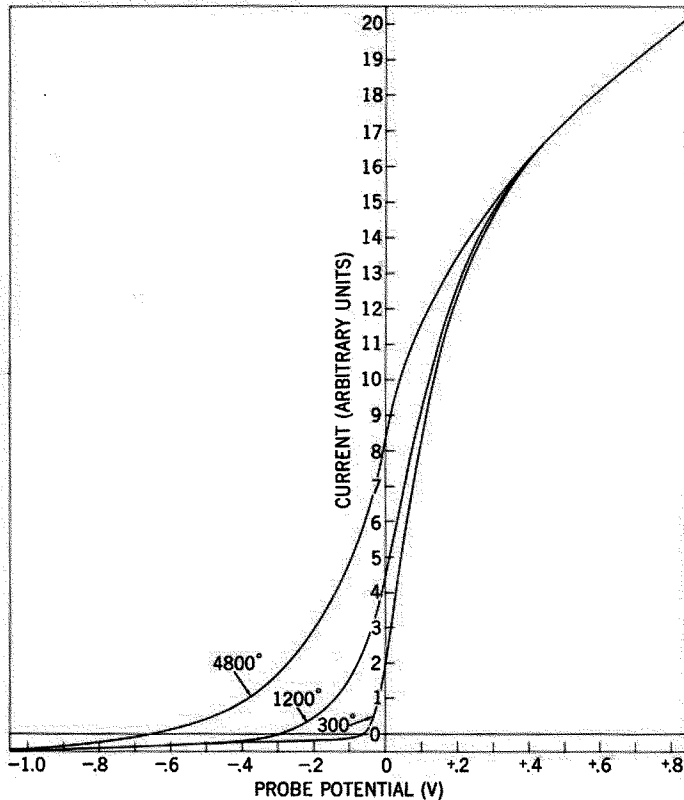


Fig. 3. Family of volt-ampere curves demonstrating the effect of  $T_e$  on the shape of the curve for a fixed  $V_A$  amplitude.

Figure 3 depicts the effect of  $T_e$  on the shape of the exponential or retarding region of the volt-ampere curve using a fixed sweep voltage slope. Because each of the curves is exponential in the electron retardation region, it is possible to adjust the slope of  $V_A$  such that the curve resulting from any value of  $T_e$  will produce a 'framed' curve.

Figure 4, a stylized schematic of a sensor with its electrometer and  $V_A$  generator, illustrates how control of the curve framing process is implemented and how  $V_A$  is applied to the guard and collector. The current to the collector is measured by the electrometer. Details of the implementation are discussed later. A properly framed curve is defined in Figure 5. We have defined, based on experience, a framed curve as having the following characteristics.

- $V_A$  peak to peak =  $10 kT_e$  ( $kT_e$  is that value of  $V_A$  which produces a change in electron current equal to a factor of  $e$ . The factor of 10 has been found to provide an adequate margin of safety, resulting in most curves being on scale).
- $V_A$  bias must be set to account for changes in  $V_s$ , independently of setting the slope of  $V_A$ .
- $I_e = 3 I_i$  (Electrometer gain, set in the ion region, produces an output voltage swing of one fourth of full scale).

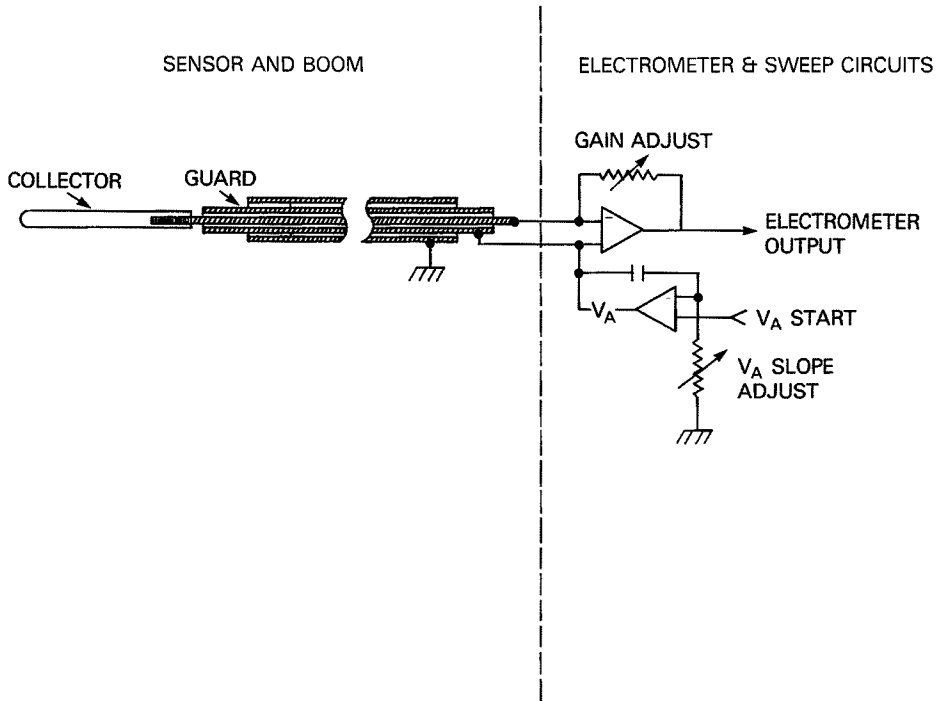


Fig. 4. Stylized schematic diagram of the collector, guard and boom connected to the electrometer amplifier and  $V_A$  generator. The variable resistors illustrate the control of the electrometer gain, the  $V_A$  Slope and the  $V_A$  Start voltage which implement the adaptive curve framing process.

– Electrometer output should first reach full scale  $8kT_e$  after sweep start. These rules permit the curve framing process to proceed adaptatively using the data obtained from curve  $N$  to frame curve  $N + 1$ .

### 3.1.1. The Adaptive Process

Figure 5 illustrates how the adaptive process causes the instrument to produce properly framed volt-ampere curves as plasma conditions change. The linear electrometer provides a positive output voltage when net electron current is collected by the sensor and a negative output when net ion current is flowing. Full scale ion current is defined at  $-3.30$  V, and full scale electron current is defined at  $+9.50$  V. The electrometer gain is set using the ion current at the beginning of each cycle ( $T_0$ ) when a fixed negative voltage ( $V_A$  start) is applied. The decade and vernier ranges converge on a gain setting that sets the output at  $-3.30$  V. The  $V_A$  is then swept positively at the rate  $V_A$  slope that was determined by the plasma conditions measured on the previous sweep. If the framing is still correct for the plasma currently encountered, this  $V_A$  slope will cause the electrometer output to rise to  $1.41$  V at the time labelled  $T_2$  and will reach  $9.50$  V at the time  $T_3$ . A one decade downrange occurs at that point to permit the rest of the curve to be placed on scale. At time  $T_4$ , a fixed step of  $+2$  V is added to the final sweep value

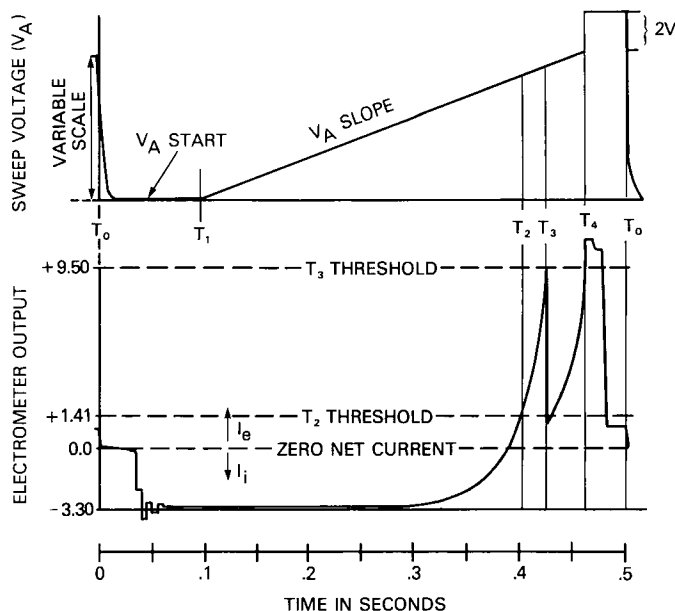


Fig. 5. An idealized volt-ampere curve illustrating when various functions occur within each 1/2 s instrument cycle when the curve is properly framed. Note that through proper selection of  $V_A$  slope the family of curves of Figure 3 can be framed as shown here. The control signals used in framing each curve are telemetered as inflight measurements of the plasma parameters.

to allow a single sample of  $I_e$  in the electron saturation region for the measurement of  $N_e$ . One sweep is performed every half second.

Since the sensors are exposed to plasma densities in the range of  $10^2$  to  $10^7$   $\text{cm}^{-3}$ , the electrometer must have a sufficient dynamic range to follow the ion current through the range of  $1 \times 10^{-10}$  to  $1 \times 10^{-5}$  A. The possible range of  $T_e$  between 300 and 20 000 K requires that the  $V_A$  amplitude be adjustable over the range of 0.2 to 17 V. Since the spacecraft potential may vary by several volts, the  $V_A$  circuitry also must sense these changes and shift the  $V_A$  bias to compensate.

When the adaptive process has occurred properly, the framed volt-ampere curves that are presented to the telemetry will appear essentially identical, regardless of changes in  $N_e$  and  $T_e$  of the ionospheric plasma. To the extent that this framing is achieved, the gain settings, sweep amplitudes and sweep biases reflect the changing values of  $N_i$ ,  $N_e$ ,  $T_e$ , and  $V_s$ . Therefore, these engineering parameters are telemetered as inflight measurements of the geophysical parameters. The advantage of these inflight data is that they permit high spatial resolution of the plasma variations without the high telemetry rate required to sample and recover the complete volt-ampere curves themselves for ground analysis. However, a small percentage of the raw volt-ampere curves are stored for ground analysis to permit verification or calibration of the inflight measurements. These are called stored curves.

### 3.2. INSTRUMENT CONTROL AND INFLIGHT DATA PROCESSING

Instrument control falls into four main categories; electrometer gain control, sweep voltage control and instrument timing and command control of operational modes.

Electrometer gain control is carried out via a successive approximation technique implemented in CMOS logic elements. The means by which gain is established and controlled can be seen from Figure 6. Gain is set at the beginning of each sweep of  $V_A$ , and the vernier gain is then fixed for the rest of the measurement cycle. The decade gain is reduced during the sweep as required to keep the curve on scale and during the  $N_e$  sample period, if necessary.

$V_A$  control is implemented in CMOS logic and operational amplifiers. The level detectors shown in Figure 6, in addition to their function of determining times  $T_2$  and  $T_3$ , are also used to trigger sample and hold circuits which measure the value of  $V_A$  at  $T_2$  and  $T_3$ . The difference in these  $V_A$  values provides the inflight measurement of  $T_e$ .

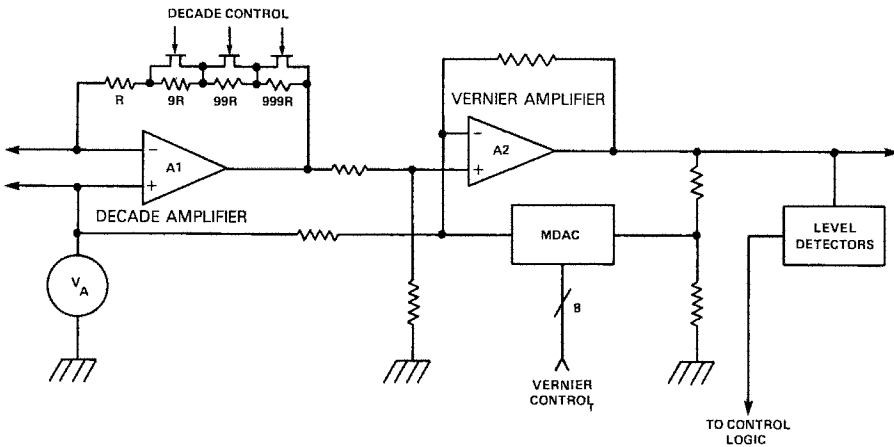


Fig. 6. A simplified schematic of the electrometer showing the means of controlling electrometer decade and vernier gain and the level detectors used in the adaptive curve framing process.

In practice, discontinuous changes in  $N_e$ ,  $V_s$ , or  $T_e$  may interfere with the adaptive process and thus initiate a default condition. For example, if the  $V_A$  at  $T_1$  does not provide a net ion current to the collector, or if the electrometer fails to reach the  $T_3$  threshold (9.50 V), the  $V_A$  generator will preset to the 'fault' condition for the next sweep, causing  $V_A$  to start at  $-10$  V and sweep to  $+7$  V. The fault sweep amplitude will usually be sufficient to locate the operating region of the volt-ampere curve and thus permit the convergence algorithm to repeat the framing processes at the beginning of the following sweep.

As a safeguard against unforeseen difficulties which might cause the adaptive approach to fail, a fixed amplitude sweep mode can be selected by ground command in which a sequence of high and low voltage sweeps are applied to either or both sensors. The high  $V_A$  is  $-7$  to  $+5$  V and the low  $V_A$  is  $-2$  to  $+1$  V. In this mode, a bias voltage of  $\pm 1$  V can be added by ground command to account for  $V_s$  changes.



The DE-LANG is equipped with two additional operational modes to provide high spatial resolution measurements of either ion or electron density. In either mode, the 1/2 s measurement interval is initiated by setting  $V_A$  equal to  $-7$  V (adjustable  $\pm 1$  V by ground command) so that the electrometer range can be adjusted using the ion current.  $V_A$  is then held fixed at either  $-7$  V to resolve the ion density structure or at  $+5$  V to resolve the electron density structure via analog telemetry channels.

### 3.3. TELEMETRY

#### 3.3.1. Digital Data

A first-in-first-out buffer stores the inflight measurements and stored curves for output to the digital telemetry system at a constant rate of 256 BPS. The 50 point stored curves are quantized with 10 bit accuracy and are used on the ground to verify the accuracy of the inflight data processing algorithms. Figure 7 is an illustration of such a stored curve from the Pioneer Venus OETP [1].

```
ORBIT 112 DAY 79085 UT 19:54:17
ALT= 323 LAT = -0.6 LONG=-157
SZA= 114 HOUR= 19.6 UANG= 17
TEMPERATURE
3330
```

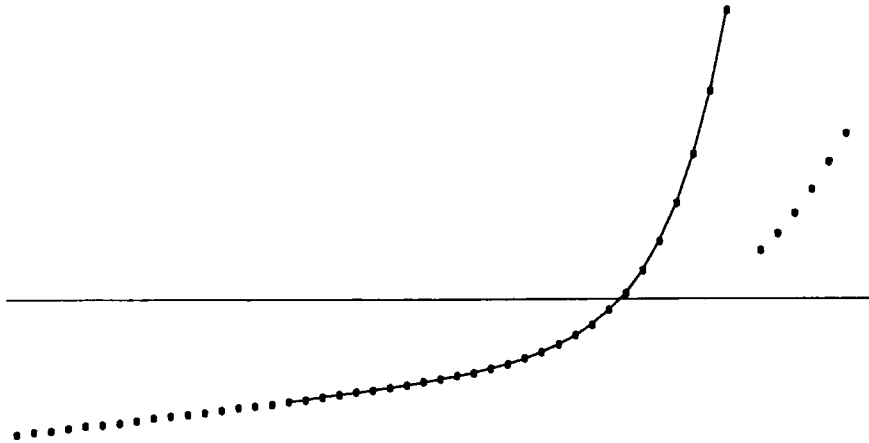


Fig. 7. Computer plot of a typical properly framed 50-point stored curve from the Pioneer Venus OETP [1]. The line, representing a fit to the electron retardation region, was performed by ground computer analysis to determine  $T_e$  as a check upon the inflight measurements.

Sixteen curves from each probe are required for a complete 8 s data cycle. Digital data can be dedicated to either of the two electrometers or time shared between them. In the dedicated modes, the inflight measurements of  $T_e$ ,  $N_e$ ,  $N_i$ , and  $V_s$  from the selected sensor, and  $T_e$  from the other sensor, are telemetered from every curve. Two stored curves from the selected sensor are also transmitted in each eight second interval. The time shared mode divides the digital data rate equally between the two electrometers producing

32 values of  $T_e$ , 16 values each of  $N_e$ ,  $N_i$ , and  $V_s$ . Also a single stored curve from each sensor is transmitted.

### 3.3.2. Analog Data

Two analog telemetry outputs can be switched, by ground command, to telemeter the output of the electrometer and  $V_A$  generator from either one of the sensors. This provides an analog data rate of 64 samples per second for the electrometer and 32 samples per second of  $V_A$ . These data are quantized by the spacecraft to eight bit accuracy and are processed by ground based computer analysis to yield values for  $T_e$ ,  $N_e$ ,  $N_i$ , and  $V_s$ . If the selected probe is being held at a fixed potential, these analog outputs are used as a high resolution measurement of  $N_e$  or  $N_i$ . This is the planned mode of operation for one of the probes. The spatial resolution in this mode is approximately 120 m along the orbit.

### 3.4. THE PROBE CLEANER

An ancillary DC power supply is provided which can be connected to the + Y sensor by ground command. Either positive or negative potentials of 150 V can be applied. Our intention is to use this power supply to drive off contaminants via ion or electron bombardment should the sensor become contaminated inflight by spacecraft outgassing or other sources.

## Acknowledgments

The authors are grateful to Jane Jellison of GSCF for her metallurgical examination of collector sections to permit an informed selection of candidate sensors. We also thank G. R. Carignan and his staff at the Space Physics Research Laboratory of the Univ. of Michigan for carrying out the necessary modifications to the Pioneer Venus instrument.

## References

1. Krehbiel, J., Brace, L., Theis, R., Cutler, J., Pinkus, W., and Kaplan, R.: *IEEE Trans. Geosci. and Rem. Sens. GE-18* 1, 49 (1980).
2. Langmuir, I. and Mott-Smith, H., Jr.: *Gen. Elec. Rev.*, 1924, p. 616.
3. Brace, L.: *Space Research X*. Amsterdam, The Netherlands, North-Holland, 1970, p. 633.
4. Brace, L., Theis, R., and Dalgarno, A.: *Radio Science* 8, 341 (1973).
5. Brace, L., Theis, R., Krehbiel, J., Nagy, A., Donahue, R., McElroy, M., and Pedersen, A.: *Science* 203, 763 (1979).
6. Brace, L., Taylor, H., Jr., Cloutier, P., Daniell, R., Jr., and Nagy, A.: *Geophys. Res. Letters* 6, 345 (1979).
7. Brace, L., Theis, R., Niemann, H., Mayr, H., Hoegy, W., and Nagy, A.: *Science* 205, 102 (1979).
8. Brace, L., Theis, R., Hoegy, W., Wolfe, J., Mihalov, J., Russell, C., Elphic, R., and Nagy, A.: *J. Geophys. Res.* 85, 7663 (1980).
9. Hoegy, W. and Wharton, L.: *J. Appl. Phys.* 44, 5365 (1973).
10. Mott-Smith, H., Jr. and Langmuir, I.: *Phys. Rev.* 28, 727 (1926).
11. Spencer, N., Brace, L., Carignan, G., Taeusch, D., and Niemann, H.: *J. Geophys. Res.* 70, 2665 (1965).
12. Smith, D.: *Planet. Space Sci.* 20, 1721 (1972).
13. Yang, L.: in F. A. Glaski, (ed.), *The Third Ann. Conf. on Chem. Vapor Dep.*, American Nuclear Society (1972).